Control Engineering Practice 19 (2011) 1099–1108

Contents lists available at ScienceDirect

Control Engineering Practice

journal homepage: www.elsevier.com/locate/conengprac

# A hierarchical controller for miniature VTOL UAVs: Design and stability analysis using singular perturbation theory

Sylvain Bertrand [a,*], Nicolas Guénard [b], Tarek Hamel [c], Hélène Piet-Lahanier [a], Laurent Eck [b]

[a] ONERA - The French Aerospace Lab, F-91761 Palaiseau, France
[b] CEA-LIST, F92265 Fontenay-aux-Roses, France
[c] I3S-UNSA-CNRS, 2000 route des Lucioles, 06903 Sophia Antipolis, France

ARTICLE INFO

*Article history:*
Received 20 August 2009
Accepted 27 May 2011
Available online 22 July 2011

*Keywords:*
Unmanned aerial vehicles
Hierarchical control
Guidance and control
Singular perturbation theory

ABSTRACT

This paper presents the design and the stability analysis of a hierarchical controller for unmanned aerial vehicles (UAV), using singular perturbation theory. Position and attitude control laws are successively designed by considering a time-scale separation between the translational dynamics and the orientation dynamics of a six degrees of freedom vertical take-off and landing (VTOL) UAV model. For the design of the position controller, we consider the case where the linear velocity of the vehicle is not measured. A partial state feedback control law is proposed, based on the introduction of a virtual state into the translational dynamics of the system. Results from simulation and from experiments on a miniature quadrirotor UAV are provided to illustrate the performance of the proposed control scheme.


## 1. Introduction

Miniature unmanned aerial vehicles (UAV) are prone to be useful for numerous military and civil applications. Especially, thanks to features such as vertical take-off and landing (VTOL) and hover capability, rotorcraft-based miniature UAVs are particularly well suited for missions such as video inspection of buildings for maintenance, road traffic supervision, victims localization after natural disasters, etc. Such vehicles have also received a growing interest from academic research institutes, since they can be used as low cost testbeds for robotic studies (Kundak & Mettler, 2007; Valenti, Bethke, Fiore, How, & Feron, 2006; Waslander, Hoffman, Jang, & Tomlin, 2005).

To make autonomous flight of miniature UAVs possible, control laws must be developed to replace the action of a human pilot. Linear control techniques such as PID or LQR have been applied to solve this problem (Bouabdallah, Noth, & Siegwart, 2004; Budiyono & Wibowo, 2007), but stability is only guaranteed in a restricted domain of flight. Input–output linearization is one of the nonlinear control schemes that have been proposed for rotary wings UAVs. Since that method can only be applied to minimum phase systems, and since, generally, helicopters have unstable zero dynamics, an approximate input–output linearization has been proposed in Koo and Sastry (1998). Another solution consists in the application of backstepping techniques, by considering the model used for control design as a chain of integrators. Backstepping has been widely applied to different miniature vehicles such as conventional helicopters (Frazzoli, Dahleh, & Feron, 2000; Mahony & Hamel, 2004), coaxial birotor helicopters (Dzul, Hamel, & Lozano, 2003) or four-rotor vehicles (Bouabdallah & Siegwart, 2005).

These two control strategies lead to a dynamical extension of the controller and make it difficult to use them in practice. Moreover, they cannot handle a time-scale separation due to different rates of measurements on the translational dynamics and on the orientation dynamics.

For practical use, a more suitable approach is the hierarchical control. In that case, separate controllers can be designed to successively stabilize the translational dynamics and the orientation dynamics of the vehicle. This method, classically known in aeronautics as guidance and control, can handle time-scale separation. Considering miniature UAVs, a hierarchical control strategy has been applied, for example, to a ducted fan miniature UAV (Pflimlin, Hamel, Souères, & Mahony, 2006).

In hierarchical control, the time-scale separation between the translational dynamics (slow time-scale) and the orientation dynamics (fast-time scale) can be used to design position and orientation controllers under simplifying assumptions. Although reduced-order subsystems can hence be considered for control design, the stability must be analyzed by considering the complete closed-loop system.

A theoretical background for time-scale separation approaches and stability analysis is provided by the singular perturbation

* Corresponding author. Tel.: +33 180386612; fax: +33 180386881.
*E-mail addresses:* sylvain.bertrand@onera.fr (S. Bertrand), nicolas.guenard@cea.fr (N. Guénard), thamel@i3s.unice.fr (T. Hamel), helene.piet-lahanier@onera.fr (H. Piet-Lahanier), laurent.eck@cea.fr (L. Eck).

0967-0661/$ - see front matter © 2011 Elsevier Ltd. All rights reserved.
doi:10.1016/j.conengprac.2011.05.008

theory (Khalil, 1992; Kokotovic, Khalil, & O'Reily, 1986). Aerospace applications of that theory can be found in Naidu and Calise (2001). In Heiges, Menon, and Schrage (1989) and Njaka and Menon (1994), a time-scale separation is considered for helicopter control design, but stability issues are not considered. A theoretical stability analysis is provided in Esteban, Gordillo, and Aracil (2007) using singular perturbation theory, for the altitude dynamics of a miniature VTOL UAV. As a complementary work of Esteban, Aracil, and Gordillo (2005), closed-loop stability is analyzed by considering a three-time-scale model of a miniature helicopter mounted on a stand, incorporating collective pitch actuator dynamics. To our knowledge, this is the only work that theoretically addresses stability issues for VTOL UAVs using singular perturbation theory. However, it only focuses on the vertical motion of the vehicle, and full state measurement is assumed to be available.

In this paper, we present the design and stability analysis of a VTOL UAV hierarchical controller using singular perturbation theory. A six degrees of freedom model is considered, based on a simplified rigid body representation of miniature VTOL UAV dynamics. The kinematic representation that we use exploits the $SO(3)$ group and its manifold. For control design, we assume that no measurement of the linear velocity of the vehicle is available. This case corresponds to the practical use of an UAV equipped with an inertial measurement unit (IMU) that provides an estimate of the attitude angles and angular velocities, and with a video camera that measures the relative position of the vehicle with respect to its environment.

The paper is organized as follows. In the next section, we introduce notations and mathematical identities that will be used in the rest of the paper. In Section 3, the UAV model and the hierarchical control strategy are presented. In Section 4, a partial state feedback position controller is designed, based on previous results (Bertrand, Hamel, & Piet-Lahanier, 2007), by introducing a virtual state in the translational dynamics, and without requiring an observer. In Section 5, the design of the attitude controller is presented, and stability of the complete closed-loop system is analyzed in Section 6. In Sections 7 and 8, simulation results and experimental results on a miniature X4-flyer VTOL UAV are, respectively, provided to illustrate the good performance of the controller. Concluding remarks are finally given at the end of the paper.

## 2. Notations and mathematical identities

Let $SO(3)$ denote the special orthogonal group of $\mathbb{R}^{3\times3}$ and $\mathfrak{so}(3)$ is the group of antisymmetric matrices of $\mathbb{R}^{3\times3}$.

We define by $(.)_\times$ the operator from $\mathbb{R}^3\to\mathfrak{so}(3)$ such that

$$\forall b\in\mathbb{R}^3, b_\times=\begin{bmatrix}0 & -b_3 & b_2\\ b_3 & 0 & -b_1\\ -b_2 & b_1 & 0\end{bmatrix} \tag{1}$$

where $b_i$ denotes the $i$th component of the vector $b$.

Let $V(.)$ be the inverse operator of $(.)_\times$, defined from $\mathfrak{so}(3)\to\mathbb{R}^3$, such that

$$\forall b\in\mathbb{R}^3,\ V(b_\times)=b \quad \forall B\in\mathfrak{so}(3),\ V(B)_\times=B \tag{2}$$

For a given vector $b\in\mathbb{R}^3$ and a given matrix $M\in\mathbb{R}^{3\times3}$, let us consider the following notations and identities:

$$P_a(M)=\frac{M-M^T}{2},\quad P_s(M)=\frac{M+M^T}{2} \tag{3}$$

$$\mathrm{tr}(P_a(M)P_s(M))=0 \tag{4}$$

$$\tfrac{1}{2}\mathrm{tr}(b_\times M)=-b^TV(P_a(M)) \tag{5}$$

The following identity will also be used:

$$\forall A_a\in\mathfrak{so}(3),\quad \tfrac{1}{2}\mathrm{tr}(A_a^TA_a)=\|V(A_a)\|^2 \tag{6}$$

Denote by $(\gamma_R,n_R)$ the angular-axis coordinates of a given matrix $R\in SO(3)$, and by $I_d$ the identity matrix of $\mathbb{R}^{3\times3}$. One has

$$\forall R\in SO(3),\quad \mathrm{tr}(I_d-R)=2(1-\cos(\gamma_R)) \tag{7}$$

$$\forall R\in SO(3),\quad \|V(P_a(R))\|=\cos\left(\frac{\gamma_r}{2}\right)\sqrt{\mathrm{tr}(I_d-R)} \tag{8}$$

Finally, for a given positive definite matrix $P\in\mathbb{R}^{3\times3}$, we denote by $\lambda_{min}(P)$ and $\lambda_{max}(P)$ the minimum and maximum modules of the eigenvalues of $P$.

## 3. UAV model and control strategy

### 3.1. Rigid body dynamics of a VTOL UAV

The VTOL UAV is represented by a rigid body of mass $m$ and tensor of inertia $I$. To describe the motion of the UAV, two reference frames are introduced: an inertial reference frame $(\mathcal{I})$ associated with the vector basis $(e_1,e_2,e_3)$ and a body frame $(\mathcal{B})$ attached to the UAV and associated with the vector basis $(e_1^b,e_2^b,e_3^b)$. The position and the linear velocity of the UAV in $(\mathcal{I})$ are, respectively, denoted $\chi=[x\ y\ z]^T$ and $v=[v_x\ v_y\ v_z]^T$. The orientation of the UAV is given by the orientation matrix $R\in SO(3)$ from $(\mathcal{I})$ to $(\mathcal{B})$, usually parameterized by Euler's pseudoangles $\psi$, $\theta$, $\phi$ (yaw, pitch, roll). Finally, let $\Omega=[\Omega_1\ \Omega_2\ \Omega_3]^T$ be the angular velocity of the UAV defined in $(\mathcal{B})$.

We assume that a translational force $F$ and a control torque $\Gamma$ are applied to the UAV. The translational force $F$ combines thrust, lift, drag and gravity components. For a miniature VTOL UAV in quasi-stationary flight we can reasonably assume that the aerodynamic forces are always in direction $e_3^b$, since the lift force predominates the other components (Hamel & Mahony, 2004). By separating the gravity component $mge_3$ from the other forces, the dynamics of the VTOL UAV can be written as

$$\begin{cases}\dot\chi=v\\ m\dot v=-\mathcal{T}Re_3+mge_3\\ \dot R=R\Omega_\times\\ I\dot\Omega=-\Omega_\times I\Omega+\Gamma\end{cases} \tag{9}$$

where the first two equations represent the translational dynamics and the last two equations describe the orientation dynamics.

The control inputs that will be considered are the scalar $\mathcal{T}\in\mathbb{R}^+$ representing the magnitude of the external forces applied in direction $e_3^b$, and the control torque $\Gamma=[\Gamma_1\ \Gamma_2\ \Gamma_3]^T$ defined in $(\mathcal{B})$.

### 3.2. Hierarchical control strategy

In this section, we consider the problem of the vehicle stabilization around a desired position $\chi^d=[x^d\ y^d\ z^d]^T$ assumed to be constant (or slowly time-varying with respect to the UAV dynamics), i.e. $\dot\chi^d=0$.

For control design, let us define the position error $\xi=\chi-\chi^d$. The system (9) becomes

$$\begin{cases}\dot\xi=v\\ m\dot v=-\mathcal{T}Re_3+mge_3\\ \dot R=R\Omega_\times\\ I\dot\Omega=-\Omega_\times I\Omega+\Gamma\end{cases} \tag{10}$$

For the stabilization of the model (10), we consider a hierarchical control strategy. Position and attitude controllers will be successively designed, as presented below.

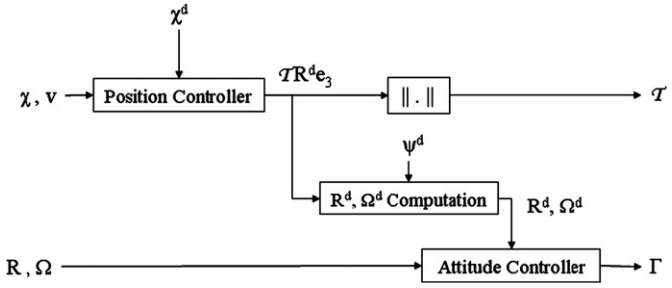


**Fig. 1.** Block diagram of the hierarchical controller.

For the translational dynamics of (10), the full vectorial term $\mathcal{T}Re_3$ will be considered as the position control vector. We will assign its desired value[1] $(\mathcal{T}Re_3)^d = f(\xi,v)$. Assuming that actuator dynamics are negligible with respect to the rigid body dynamics of the UAV, the value $\mathcal{T}^d$ is considered to be instantaneously reached by $\mathcal{T}$. Therefore, we have $(\mathcal{T}Re_3)^d = \mathcal{T}R^de_3$, where $R^d$ is the desired orientation of the vehicle. Note that this vector can be split into its magnitude, $\mathcal{T} = \|f(\xi,v)\|$, representing the first control input, and its direction

$$R^de_3 = \frac{1}{\mathcal{T}}f(\xi,v) \tag{11}$$

The desired orientation $R^d$ can then be deduced from (13), by using its pseudo-Euler angle parametrization and solving for $(\psi^d,\theta^d,\phi^d)$ for a given specified constant yaw $\psi^d(t) = \psi^d(0)$ (Hamel, Mahony, Lozano, & Ostrowski, 2002).

For the orientation dynamics of (10), we will assign the control torque $\Gamma$ such that the orientation $R$ of the UAV converges to the desired orientation $R^d$, and such that the angular velocity $\Omega$ converges to $\Omega^d$ defined by

$$\dot{R}^d = R^d\Omega^d_\times \tag{12}$$

The computation of the desired angular velocity $\Omega^d$ is presented in Appendix A.

A block diagram of the hierarchical controller is provided in Fig. 1.

### 3.3. Time-scale separation

The classical way to design guidance and control laws in aeronautics consists in assuming that the controllers will be tunned such that the closed-loop attitude dynamics would converge faster than the closed-loop translational dynamics (by using for example a 'high gain' attitude controller). Hence the complete closed-loop system will be stable in practice. In this paper, we would like to quantify how 'high' the gains of the attitude controller should be to theoretically ensure the closed-loop stability of the whole system.

A way to do that is to consider that the problem can also be seen in the context of a time-scale separation between the translational and the orientation dynamics, one closed-loop subsystem converging faster than the other one. Therefore, the control laws can be designed by using simplifying assumptions linked to the time-scale separation approach:

- for the design of the position control law, it can be assumed that the orientation dynamics converge faster than the translational dynamics, and hence one can consider $R = R^d$,
- for the design of the attitude control law, it can be assumed that the translational dynamics converge slower than the orientation dynamics, and hence one can assume $\Omega^d = 0$ ($R^d = cste$).

[1] In this paper, the function $f$ will not depend on $v$, since only position measurements are available for the control of the translational dynamics.

Note that the stability analysis of the complete closed-loop system has to be proved without considering these two simplifying assumptions. A good framework to formalize this time-scale separation and to get conditions on it for stability is provided by the singular perturbation theory.

The scale parameter $\varepsilon \in (0,1]$ is introduced in that way to formalize the time-scale separation. Multiplying by $\varepsilon$ the orientation dynamics equations of (10), we get

$$\begin{cases} \dot{\xi} = v \\ m\dot{v} = -\mathcal{T}Re_3 + mge_3 \\ \varepsilon\dot{R} = \varepsilon R\Omega_\times \\ \varepsilon I\dot{\Omega} = -\varepsilon\Omega_\times I\Omega + \varepsilon\Gamma \end{cases} \tag{13}$$

Introducing the notations

$$\omega = \varepsilon\Omega, \quad \omega^d = \varepsilon\Omega^d, \quad \gamma = \varepsilon\Gamma \tag{14}$$

the system (15) can be restated as

$$\begin{cases} \dot{\xi} = v \\ m\dot{v} = -\mathcal{T}Re_3 + mge_3 \\ \varepsilon\dot{R} = R\omega_\times \\ \varepsilon I\dot{\Omega} = -\omega_\times I\Omega + \gamma \end{cases} \tag{15}$$

System (15) is the one that will be considered for control design. Note that it is strictly equivalent to system (10). Hence, designing control laws for the inputs $\mathcal{T}$ and $\Gamma$ of (10) can be achieved by designing control laws for the inputs $\mathcal{T}$ and $\gamma$ of (15).

## 4. Position controller

Consider the translational dynamics of (15). We assume for control design that only measurements on the position $\xi$ are available. In that case, partial state feedback control strategies (Burg, Dawson, Hu, & de Queiroz, 1996; Burg, Dawson, & Vedagarbha, 1997; Dixon, Zergeroglu, Dawson, & Hannan, 2000) can be used to deal with the lack of velocity measurements without requiring the use of an observer. In this section, a partial state feedback position controller is proposed, based on the introduction of a virtual state in the translational dynamics of the system.

Let us introduce a virtual state $q \in \mathbb{R}^3$ and a virtual input $\delta \in \mathbb{R}^3$ such that

$$\begin{cases} \dot{\xi} = v \\ \dot{v} = -\dfrac{\mathcal{T}}{m}R^de_3 + ge_3 - \dfrac{\mathcal{T}}{m}(R - R^d)e_3 \\ \dot{q} = \delta \end{cases} \tag{16}$$

Introducing the notation

$$\alpha = \xi - q \tag{17}$$

we define the position control law

$$\mathcal{T}R^de_3 = m\{k_x\xi + k_1\alpha\} + mge_3 \tag{18}$$

and the virtual input

$$\delta = \alpha \tag{19}$$

where $k_x$ and $k_1$ are strictly positive gains.

**Remark 1.** Note that the controller (18) and the virtual input (19) do not require measurements on the linear velocity $v$ of the vehicle.

**Remark 2.** The control law (18) and the virtual input (19) have been designed by considering the translational dynamics (16) under the assumption $R = R^d$. As previously mentioned in Section 3.3, this

assumption corresponds to a time-scale separation between the translational dynamics and the orientation dynamics.

Introducing the notations

$$u=-\frac{\mathcal{T}}{m}Re_3+ge_3,\quad u^d=-\frac{\mathcal{T}}{m}R^de_3+ge_3,\quad \tilde{u}=u-u^d \tag{20}$$

the system (16) controlled by (18) along with (19) can be written as

$$\begin{cases}\dot{\xi}=v\\ \dot{v}=-k_x\xi-k_1\alpha+\tilde{u}\\ \dot{\alpha}=v-\alpha\end{cases} \tag{21}$$

Defining the vectors $X=[\xi^T\ v^T\ \alpha^T]^T$ and $\tilde{U}=[0_3^T\ \tilde{u}^T\ 0_3^T]^T$, with $0_3=[0\ 0\ 0]^T$, the system (21) can be represented by

$$\dot{X}=AX+\tilde{U} \tag{22}$$

where the matrix $A\in\mathbb{R}^{9\times9}$ is Hurwitz.[2] Therefore, the system (22) is exponentially stable for $\tilde{U}=0$. In that case, there exist two positive definite symmetric matrices $P\in\mathbb{R}^{9\times9}$ and $Q\in\mathbb{R}^{9\times9}$ verifying the Lyapunov equation

$$\tfrac{1}{2}(A^TP+PA)=-Q \tag{23}$$

and such that we can define a control Lyapunov function

$$\mathcal{S}=\tfrac{1}{2}X^TPX \tag{24}$$

which verifies

$$\tfrac{1}{2}\lambda_{min}(P)\|X\|^2\le\mathcal{S}\le\tfrac{1}{2}\lambda_{max}(P)\|X\|^2 \tag{25}$$

$$\dot{\mathcal{S}}=-X^TQX\le-\lambda_{min}(Q)\|X\|^2 \tag{26}$$

Consider now the case $\tilde{U}\neq0$. The time derivative of $\mathcal{S}$ along the trajectories of (22) becomes

$$\dot{\mathcal{S}}=-X^TQX+\tilde{U}^TPX \tag{27}$$

The above expression can be bounded by

$$\dot{\mathcal{S}}\le-\lambda_{min}(Q)\|X\|^2+\lambda_{max}(P)\|\tilde{u}\|\{\|\xi\|+\|v\|+\|\alpha\|\} \tag{28}$$

To determine an upper bound on $\|\tilde{u}\|$ we compute

$$\|\tilde{u}\|=\frac{\mathcal{T}}{m}\|(R-R^d)e_3\|=\frac{\mathcal{T}}{m}\|(R^dR^T-I_d)Re_3\| \tag{29}$$

$$\|\tilde{u}\|\le\frac{\mathcal{T}}{m}\sqrt{\mathrm{tr}((R^dR^T-I_d)^T(R^dR^T-I_d))}\|Re_3\| \tag{30}$$

Introducing

$$\tilde{R}=(R^d)^TR \tag{31}$$

we get

$$\|\tilde{u}\|\le\frac{\mathcal{T}}{m}\sqrt{2\mathrm{tr}(I_d-\tilde{R})} \tag{32}$$

Let $(\gamma_{\tilde{R}},n_{\tilde{R}})$ denote the angular-axis coordinates of $\tilde{R}$. Using identity (8), we obtain

$$\|\tilde{u}\|\le\frac{\sqrt{2}}{m}\frac{\mathcal{T}}{\cos\left(\frac{\gamma_{\tilde{R}}}{2}\right)}\|V(P_a(\tilde{R}))\| \tag{33}$$

From (28), we finally get

$$\dot{\mathcal{S}}\le-\lambda_{min}(Q)\{\|\xi\|^2+\|v\|^2+\|\alpha\|^2\}+\left(\sqrt{2}\frac{\mathcal{T}}{m}\frac{\lambda_{max}(P)}{\cos\left(\frac{\gamma_{\tilde{R}}}{2}\right)}\right)\|V(P_a(\tilde{R}))\|\{\|\xi\|+\|v\|+\|\alpha\|\} \tag{34}$$

[2] Using the fact that the gains $k_x$ and $k_1$ are strictly positive, it can be easily checked that the matrix $A$ is Hurwitz, by applying Routh's criterion on its characteristic polynomial.

## 5. Attitude controller

Let us now consider the orientation dynamics of (15) and recall the notation introduced in (31):

$$\tilde{R}=(R^d)^TR \tag{35}$$

The orientation dynamics can be rewritten as

$$\begin{cases}\varepsilon\dot{\tilde{R}}=-\varepsilon\Omega^d_\times\tilde{R}+\tilde{R}\omega_\times\\ \varepsilon I\dot{\Omega}=-\omega_\times I\Omega+\gamma\end{cases} \tag{36}$$

We introduce

$$\tilde{\Omega}=\omega-l_1V(P_a(\tilde{R})^T) \tag{37}$$

where $l_1$ is a strictly positive scalar gain. With this notation, the kinematic relation can be transformed into

$$\dot{\tilde{R}}=-\Omega^d_\times\tilde{R}+\frac{1}{\varepsilon}\tilde{R}\tilde{\Omega}_\times+\frac{l_1}{\varepsilon}\tilde{R}P_a(\tilde{R})^T \tag{38}$$

Taking the time derivative of $\tilde{\Omega}$ it yields

$$\dot{\tilde{\Omega}}=I^{-1}(-\omega_\times I\Omega+\gamma)-\frac{l_1}{2}V(\tilde{R}^T\Omega^d_\times+\Omega^d_\times\tilde{R})+\frac{l_1}{2\varepsilon}V(\omega_\times\tilde{R}^T+\tilde{R}\omega_\times) \tag{39}$$

Let us define $l>0$ and $l_2>0$, and assign the following expression to the input $\gamma$:

$$\gamma=\omega_\times I\Omega+I\left(-\frac{l_2}{\varepsilon}\tilde{\Omega}-\frac{2l}{\varepsilon}V(P_a(\tilde{R}))-\frac{l_1}{2\varepsilon}V(\omega_\times\tilde{R}^T+\tilde{R}\omega_\times)\right) \tag{40}$$

The control torque $\Gamma$ can then be directly deduced from (40):

$$\Gamma=\Omega_\times I\Omega+I\left(-\frac{l_2}{\varepsilon^2}\tilde{\Omega}-\frac{2l}{\varepsilon^2}V(P_a(\tilde{R}))-\frac{l_1}{2\varepsilon}V(\Omega_\times\tilde{R}^T+\tilde{R}\Omega_\times)\right) \tag{41}$$

Eq. (39) becomes

$$\dot{\tilde{\Omega}}=-\frac{l_2}{\varepsilon}\tilde{\Omega}-2\frac{l}{\varepsilon}V(P_a(\tilde{R}))-\frac{l_1}{2}V(\tilde{R}^T\Omega^d_\times+\Omega^d_\times\tilde{R}) \tag{42}$$

**Remark 3.** The input (40), and hence the control law (41), has been designed by considering the orientation dynamics (36) under the assumption $\Omega^d=0$. This corresponds to a time-scale separation between the translational and the orientation dynamics, as previously mentioned in Section 3.3.

**Remark 4.** Note that the parameter $\varepsilon\in(0,1]$, which has been introduced to formalize the time-scale separation for control design, can also be seen as a high gain tunning parameter in the control law (41).

Let $\mathcal{L}$ be a candidate control Lyapunov function for the orientation dynamics (36):

$$\mathcal{L}=l\mathrm{tr}(I_d-\tilde{R})+\tfrac{1}{2}\|\tilde{\Omega}\|^2 \tag{43}$$

Using relations (38) and (42), and identities (4) and (5) to compute the time derivative of $\mathcal{L}$ along the trajectories of (36) controlled by (41), we get

$$\dot{\mathcal{L}}=-2l(\Omega^d)^TV(P_a(\tilde{R}))-\frac{ll_1}{\varepsilon}\mathrm{tr}(P_a(\tilde{R})P_a(\tilde{R})^T)-\frac{l_2}{\varepsilon}\|\tilde{\Omega}\|^2-\frac{l_1}{2}\tilde{\Omega}^TV(\tilde{R}^T\Omega^d_\times+\Omega^d_\times\tilde{R}) \tag{44}$$

By triangular inequality and applying identity (6), we obtain

$$\dot{\mathcal{L}} \le 2l\|\Omega^d\|\|V(P_a(\tilde{R}))\| - \frac{2ll_1}{\varepsilon}\|V(P_a(\tilde{R}))\|^2 - \frac{l_2}{\varepsilon}\|\tilde{\Omega}\|^2 + \frac{l_1}{2}\|\tilde{\Omega}\|\|V(\tilde{R}^T\Omega^d_\times + \Omega^d_\times\tilde{R})\| \quad (45)$$

To get an upper bound on $\mu = \|V(\tilde{R}^T\Omega^d_\times + \Omega^d_\times\tilde{R})\|$, we compute

$$\mu^2 \le \tfrac{1}{2}\mathrm{tr}\{(\tilde{R}^T\Omega^d_\times + \Omega^d_\times\tilde{R})^T(\tilde{R}^T\Omega^d_\times + \Omega^d_\times\tilde{R})\} \quad (46)$$

$$\mu^2 \le \tfrac{1}{2}\,\mathrm{tr}((\tilde{R}^T\Omega^d_\times)^T\tilde{R}^T\Omega^d_\times) + \tfrac{1}{2}\mathrm{tr}((\Omega^d_\times\tilde{R})^T\Omega^d_\times\tilde{R}) \quad (47)$$

$$\mu^2 \le \mathrm{tr}((\Omega^d_\times)^T\Omega^d_\times) \le 2\|\Omega^d\|^2 \quad (48)$$

It remains to find an upper bound on $\|\Omega^d\|$. In the case of stabilization, we choose $\Omega^d_3 = 0$. We get $\|\Omega^d\| = \|\Omega^d_\times e_3\|$ and can use (A.8) along with the time derivative of (18) to obtain

$$\|\Omega^d\| \le \frac{m}{\mathcal{T}}\{(k_x+k_1)\|v\| + k_1\|\alpha\|\} \quad (49)$$

Using (48) and (49) along with (45) leads finally to the following upper bound on the time derivative of $\mathcal{L}$:

$$\dot{\mathcal{L}} \le -\frac{2ll_1}{\varepsilon}\|V(P_a(\tilde{R}))\|^2 - \frac{l_2}{\varepsilon}\|\tilde{\Omega}\|^2 + \frac{2m}{\mathcal{T}}l\|V(P_a(\tilde{R}))\|\{(k_x+k_1)\|v\| + k_1\|\alpha\|\} + \frac{\sqrt{2}}{2}\frac{m}{\mathcal{T}}l_1\|\tilde{\Omega}\|\{(k_x+k_1)\|v\| + k_1\|\alpha\|\} \quad (50)$$

## 6. Stability analysis

Consider now the complete system composed of the translational dynamics (16) and of the orientation dynamics (36), and define the candidate control Lyapunov function

$$\mathcal{V} = \mathcal{S} + \mathcal{L} \quad (51)$$

We have the following proposition:

**Proposition 1.** *Consider the system* (16)–(36) *along with the control laws* (18) *and* (41) *and the virtual input* (19).

*There exist* $K_1, K_2 > 0$ *and* $\varepsilon^* > 0$ *such that, for all initial conditions* $\xi(0)$, $v(0)$, $q(0) = \xi(0)$, $R(0)$ *and* $\Omega(0)$ *such that*

$$\mathcal{V}(0) < \frac{K_2\left(g - \frac{\varepsilon_g}{m}\right)^2}{2(2K_1)^2} \quad (0 < \varepsilon_g \ll mg) \quad (52)$$

*then, for all* $l$ *verifying*

$$l \ge \frac{K_2\left(g - \frac{\varepsilon_g}{m}\right)^2}{2(2K_1)^2(4-\eta)} \quad (0 < \eta < 4) \quad (53)$$

*and for all* $\varepsilon > 0$ *such that* $\varepsilon < \varepsilon^*$, *the closed-loop system is exponentially stable.*

**Proof.** First, let us consider the following assumptions that will be verified at the end of the proof:

**Assumption 1.** There exist two reals $\mathcal{T}_{min}$ and $\mathcal{T}_{max}$ such that

$$0 < \mathcal{T}_{min} < mg < \mathcal{T}_{max} < \infty \quad (54)$$

$$\forall t \ge 0, \quad \mathcal{T}_{min} \le \mathcal{T}(t) \le \mathcal{T}_{max} \quad (55)$$

**Assumption 2.** There exists a real $c > 0$ such that

$$\forall t \ge 0, \quad \cos\left(\frac{\gamma_{\tilde{R}}(t)}{2}\right) \ge c \quad (56)$$

Let us define the coefficients

$$s_1 = \frac{1}{2}\lambda_{max}(P)\frac{\mathcal{T}_{max}}{m}\frac{\sqrt{2}}{c}, \quad s_2 = l\frac{m}{\mathcal{T}_{min}} \quad (57)$$

$$s_3 = \frac{\sqrt{2}}{4}l_1\frac{m}{\mathcal{T}_{min}} \quad (58)$$

With these notations and under Assumptions (1) and (2), we can use relations (34) and (50), to provide the following upper bound on the time derivative of $\mathcal{V}$, computed along the trajectories of (16) along with (36) controlled by (18), (41) and (19):

$$\dot{\mathcal{V}} \le -\lambda_{min}(Q)\{\|\xi\|^2 + \|v\|^2 + \|\alpha\|^2\} - \frac{2ll_1}{\varepsilon}\|V(P_a(\tilde{R}))\|^2 - \frac{l_2}{\varepsilon}\|\tilde{\Omega}\|^2 + 2s_1\|\xi\|\|V(P_a(\tilde{R}))\| + 2(s_1+s_2(k_x+k_1))\|v\|\|V(P_a(\tilde{R}))\| + 2(s_1+s_2k_1)\|\alpha\|\|V(P_a(\tilde{R}))\| + 2s_3(k_x+k_1)\|v\|\|\tilde{\Omega}\| + 2s_3k_1\|\alpha\|\|\tilde{\Omega}\| \quad (59)$$

Let us define

$$a = \lambda_{min}(Q), \quad b_1 = s_1, \quad b_2 = s_1 + s_2(k_x+k_1) \quad (60)$$

$$b_3 = s_1 + s_2k_1, \quad b_4 = s_3(k_x+k_1), \quad b_5 = s_3k_1 \quad (61)$$

and introduce the state vector

$$\mathcal{X} = [\|\xi\| \ \|v\| \ \|\alpha\| \ \|V(P_a(\tilde{R}))\| \ \|\tilde{\Omega}\|]^T \quad (62)$$

With these notations, Eq. (59) can be restated as

$$\dot{\mathcal{V}} \le -\mathcal{X}^T\Sigma\mathcal{X} \quad (63)$$

with

$$\Sigma = \begin{bmatrix} a & 0 & 0 & -b_1 & 0 \\ 0 & a & 0 & -b_2 & -b_4 \\ 0 & 0 & a & -b_3 & -b_5 \\ -b_1 & -b_2 & -b_3 & \frac{2ll_1}{\varepsilon} & 0 \\ 0 & -b_4 & -b_5 & 0 & \frac{l_2}{\varepsilon} \end{bmatrix} \quad (64)$$

Since the matrix $Q$ is positive definite, the coefficient $a = \lambda_{min}(Q)$ is strictly positive and the three first minors of the matrix $\Sigma$ are strictly positive. The positivity of the minor of size four is obtained for all $\varepsilon < \varepsilon_1^*$ with

$$\varepsilon_1^* = \frac{2\lambda_{min}(Q)ll_1}{3s_1^2 + s_2^2(2k_1^2 + k_x^2 + 2k_xk_1) + 2s_1s_2(k_x+2k_1)} \quad (65)$$

The strict positivity of $\det(\sigma)$ is obtained for

$$A\varepsilon^2 + B\varepsilon + C > 0 \quad (66)$$

where

$$A = (b_2b_5 - b_3b_4)^2 + b_1^2(b_5^2 + b_4^2) > 0 \quad (67)$$

$$B = -a[l_2(b_1^2 + b_2^2 + b_3^2) + 2ll_1(b_4^2 + b_5^2)] < 0 \quad (68)$$

$$C = 2a^2ll_1l_2 > 0 \quad (69)$$

With these coefficients, it can be checked that the discriminant $(B^2 - 4AC)$ of (66) is strictly positive. Let us define

$$\varepsilon_2^* = -B - \frac{\sqrt{B^2 - 4AC}}{2A} \quad (70)$$

Since $A > 0$, $B < 0$, $C > 0$ and $(B^2 - 4AC) > 0$, we have $\sqrt{B^2 - 4AC} < \sqrt{B^2} = -B$, and we can check the strict positivity of $\varepsilon_2^*$.

Therefore, $\det(\Sigma)$ is strictly positive for all $\varepsilon < \varepsilon_2^*$.

Let us define

$$\varepsilon^* = \min(\varepsilon_1^*, \varepsilon_2^*) \quad (71)$$

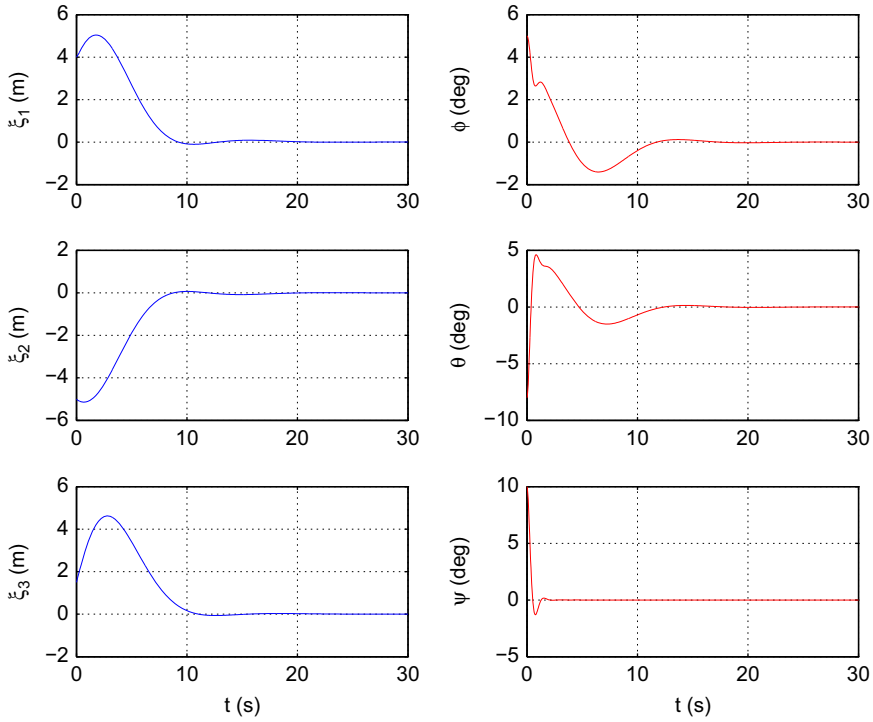


**Fig. 2.** Position error components and attitude angles.

For all $\varepsilon > 0$ such that $\varepsilon < \varepsilon^*$, the matrix $\Sigma$ is positive definite and hence the time derivative (63) of $\mathcal{V}$ is negative definite. Consequently, one can ensure the exponential stability of the system (16) along with (36) when (18) and (41) are used as control inputs and (19) as virtual control.[3]

**Remark 5.** The exponential stability is obtained by considering identity (8) from which one can deduce $\|V(P_a(\tilde{R}))\|^2 \leq \mathrm{tr}(I_d - \tilde{R})$. Defining the vector $\mathcal{X}' = [\|\xi\| \ \|v\| \ \|\alpha\| \ \sqrt{\mathrm{tr}(I_d - \tilde{R})} \ \|\tilde{\Omega}\|]^T$ and using (63) along with the fact that $\Sigma$ is positive definite, one can show that there exists a positive definite matrix $\Sigma' = \Sigma'^T$ such that $\dot{\mathcal{V}} \leq -\mathcal{X}'^T \Sigma' \mathcal{X}'$. Hence there exists a scalar $s' \in \mathbb{R}^+$ such that $\dot{\mathcal{V}} \leq -s'\mathcal{V}$ which proves the exponential stability.

We have shown that closed-loop stability is guaranteed for all $\varepsilon < \varepsilon^*$ under Assumptions 1 and 2. Now we have to check that both assumptions are satisfied.

Let us start with Assumption 1. Define $K_1 = \max(k_x, k_1)$.

Using triangular inequality with (18) yields

$$mg - mK_1(\|\xi\| + \|\alpha\|) \leq \mathcal{T} \leq mg + mK_1(\|\xi\| + \|\alpha\|) \tag{72}$$

That expression can be linked to the value of the Lyapunov function $\mathcal{V}$ using (24), (25) and (51) to get for all $t \geq 0$:

$$mg - 2mK_1\sqrt{\frac{2\mathcal{V}(t)}{K_2}} \leq \mathcal{T}(t) \leq mg + 2mK_1\sqrt{\frac{2\mathcal{V}(t)}{K_2}} \tag{73}$$

with $K_2 = \lambda_{min}(P)$.

The time derivative of $\mathcal{V}$ being negative for $\varepsilon < \varepsilon^*$, one has

$$\forall t \geq 0, \quad \mathcal{V}(t) \leq \mathcal{V}(0) \tag{74}$$

and from (73), we obtain for all $t \geq 0$:

$$mg - 2mK_1\sqrt{\frac{2\mathcal{V}(0)}{K_2}} \leq \mathcal{T}(t) \leq mg + 2mK_1\sqrt{\frac{2\mathcal{V}(0)}{K_2}} \tag{75}$$

Taking $\varepsilon_g > 0$ such that $\varepsilon_g \ll mg$, we can use condition (52) to finally get

$$\forall t \geq 0, \quad 0 < \varepsilon_g < \mathcal{T}(t) < 2mg - \varepsilon_g \tag{76}$$

Assumption 1 is hence verified by choosing $\mathcal{T}_{min} = \varepsilon_g$ and $\mathcal{T}_{max} = 2mg - \varepsilon_g$.

To complete the proof, let us finally check that Assumption 2 is verified. As previously, we use the fact that $\mathcal{V}$ is decreasing, with (43) and (51), to obtain

$$\forall t \geq 0, \quad l\mathrm{tr}(I_d - \tilde{R}(t)) \leq \mathcal{V}(t) \leq \mathcal{V}(0) \tag{77}$$

Defining $\eta > 0$ such that $\eta < 4$, conditions (52) and (53) can be used successively to get

$$\mathcal{V}(0) < (4 - \eta)l \tag{78}$$

and then

$$\forall t \geq 0, \quad \mathrm{tr}(I_d - \tilde{R}(t)) < 4 - \eta \tag{79}$$

Using (7) we obtain

$$\forall t \geq 0, \quad (1 - \cos(\gamma_{\tilde{R}}(t))) < 2 \tag{80}$$

Therefore, for all $t \geq 0$, we have $-\pi < \gamma_{\tilde{R}}(t) < \pi$ and there exists a $c > 0$ such that

$$\cos\left(\frac{\gamma_{\tilde{R}}(t)}{2}\right) \geq c > 0 \tag{81}$$

Assumption 2 is hence verified, which completes the proof. □

**Remark 6.** Since (54) and (55) are verified, the strict positivity of the input $\mathcal{T}$ is guaranteed. Therefore, the direction $R^d e_3$ computed by (11) is well defined.

**Remark 7.** Condition (52) is not restrictive. Indeed, in practice, the gains $k_x$, $k_1$ and the matrix $P$ can be chosen to obtain,

[3] The convergence of $\tilde{R}$ to the identity matrix $I_d$ is guaranteed by conditions (52) and (53) from which we can show that $(1 - \cos(\gamma_{\tilde{R}})) < 2$ and hence $\gamma_{\tilde{R}} \to 0$. This relation will be shown in the next step of the proof.

respectively, sufficient small and high values for $K_1$ and $K_2$, so that all initial conditions in the usual domain of flight of the vehicle will satisfy (52).

**Remark 8.** The design of the partial state feedback control law for the translational dynamics can also be achieved by introducing two virtual states (Bertrand et al., 2007). In that case, the corresponding complete proof can be found in Bertrand, Hamel, and Piet-Lahanier (2008).

## 7. Simulation results

Simulation results are provided in this section to illustrate the stability property of the proposed controller. The following values have been chosen for the parameters of the controller and UAV model: $k_x = 0.1$, $k_1 = 0.41$, $l = 0.77$, $l_1 = 0.75$, $l_2 = 0.26$, $\varepsilon = 0.3$, $m = 2.5$ kg, $I = \mathrm{diag}(I_1, I_2, I_3)$ with $I_1 = I_2 = 0.13$ kg m$^2$ and $I_3 = 0.16$ kg m$^2$. The gravitational acceleration is $g = 9.81$ m s$^{-2}$.

The proposed results have been obtained for stabilization at hover around the desired position $\chi^d = [0\ 0\ 1]^T$ m, starting from the initial condition $\chi(0) = [4\ -5\ 2.5]^T$ m, $[\phi(0)\ \theta(0)\ \psi(0)] = [5\ -8\ 10]^\circ$, $v(0) = [0.7\ -0.5\ 2]^T$ m/s, $\Omega(0) = 0$. The initial value chosen for the virtual state is $q(0) = \xi(0)$. The desired yaw $\psi^d$ has been chosen to be equal to zero.

Fig. 2 presents the evolution of the components of the position error $\xi = [\xi_1\ \xi_2\ \xi_3]^T$ and of the attitude angles. As can be seen, closed-loop stability is achieved by the controller with a good performance. Control inputs are shown in Fig. 3. The evolutions of the angular deviation terms $\tilde{\phi} = \phi - \phi^d$, $\tilde{\theta} = \theta - \theta^d$, $\tilde{\psi} = \psi - \psi^d$ are presented in Fig. 4. These terms converge faster than the closed-loop of the translational dynamics, hence validating the time-scale separation that has been used in the control strategy.

## 8. Experimental results

The proposed control strategy has been tested at CEA on an 'X4-flyer' miniature UAV presented in Fig. 5. This four-rotor VTOL vehicle is particularly suited for stationary or quasi-stationary flight conditions.

In a previous work, control laws have been designed for attitude stabilization from inertial measurement unit (IMU) data (Guenard, Hamel, & Eck, 2006). In order to embed the attitude stabilization algorithm, the prototype is equipped with a set of four electronic boards. The first two ones, respectively, integrate the motors controller and the IMU. On the third board, a digital signal processing (DSP) cadenced at 150 MIPS performs the attitude control algorithm computations at about 166 Hz. The last board supplies a numerical wireless communication of 2 and 4 GHz between the vehicle and a ground station (Pentium IV PC). The operator's joystick, used for the teleoperation of the UAV, is linked to this PC. An embedded camera with a view angle of 120° pointing directly down, transmits video images to the ground station via a wireless analogical link of 5.8 GHz. A lithium-polymer battery provides nearly 20 min of flight time. The payload of the prototype is about 200 g. The structure of the experimental setup is summarized in Fig. 6.

For the considered experiment, the position of the UAV is obtained by a particle filter implemented on the ground station.

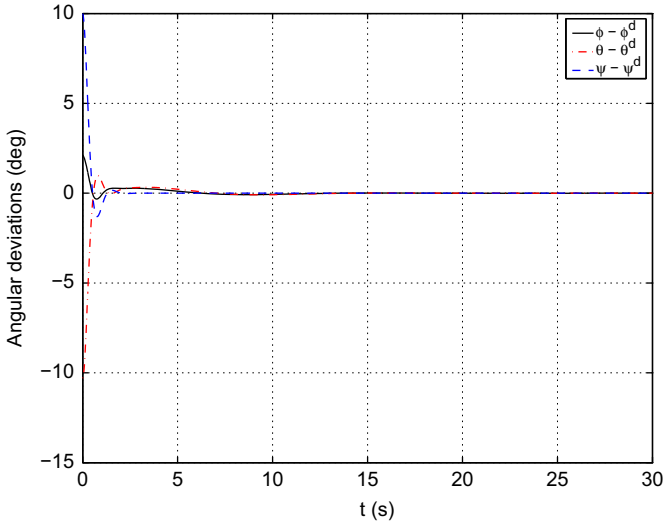


**Fig. 4.** Angular deviation terms.

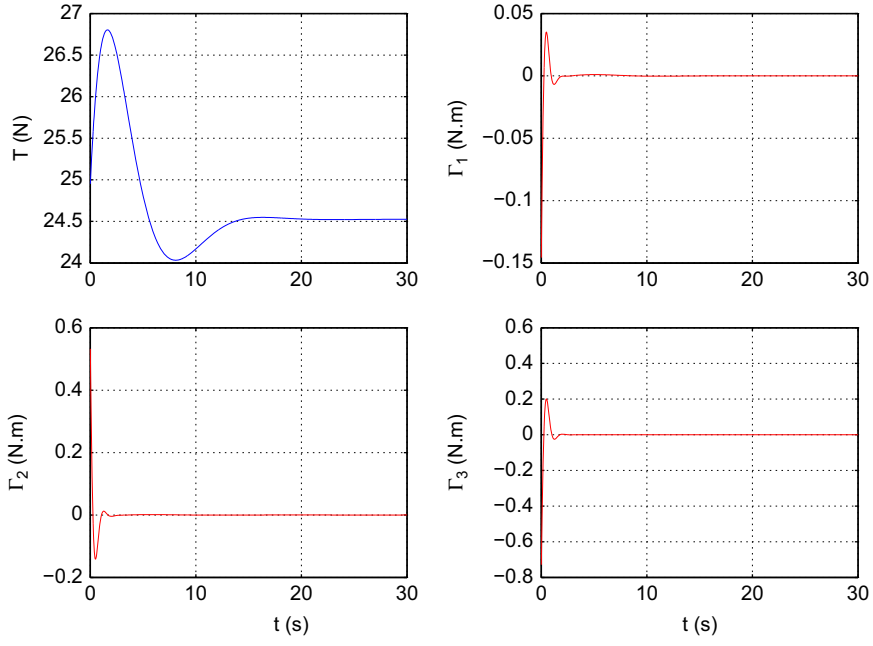


**Fig. 3.** Control inputs.

**Fig. 5.** The X4-flyer.

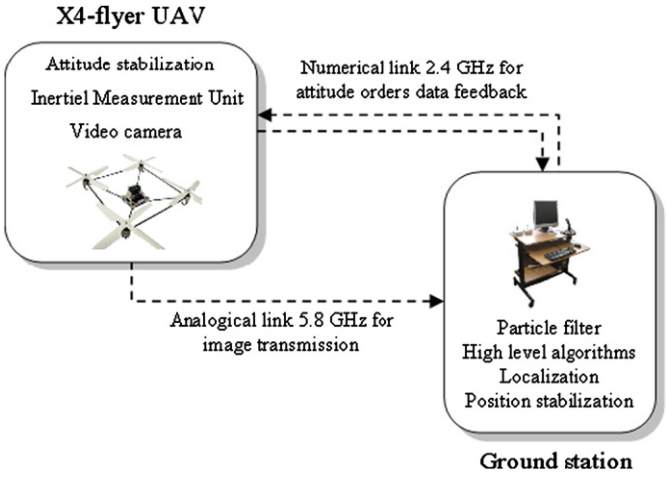


**Fig. 6.** Experimental setup architecture.

This filter uses images sent during the flight by the embedded camera and data from the IMU measurements. Images received by the ground station are also used to build a topological map of the ground, by successively defining key images from the gradient image. The position of the UAV in this map is hence defined relatively to the current tracked key image. IMU measurements are also used to compute the attitude of the vehicle and its angular velocities. Note that no linear velocity estimate is used for the control algorithm during the experiment.

The proposed position control law has been implemented on the ground station with a sample time of about 70 ms. From the vehicle position, it computes attitude orders to be sent to the UAV. Control gains have been chosen to obtain a good trade-off between the stability of the system and a fast transient response, and to ensure that the orientation dynamics converge faster than the translational dynamics, according to the chosen time-scale separation approach.

The proposed results correspond to the stabilization of the UAV around set points given by the operator and for a constant desired yaw $\psi^d$. Fig. 7 presents the position coordinates (solid curves) and the corresponding references (dashed curves). The position error $\xi$ is also represented. The evolution of the attitude angles during the flight is provided in Fig. 8. As can be seen, good performance is achieved by the proposed controller for the stabilization of the UAV. Note that the precision in the $z$-coordinate is limited by the use of vision.

## 9. Conclusion

In this paper, we have presented both design and stability analyzes of a hierarchical controller for a miniature VTOL UAV. Position and attitude controllers have been designed considering successively, and with a time-scale separation, the translational dynamics and the orientation dynamics of a six degrees of freedom VTOL UAV model. A partial state feedback controller

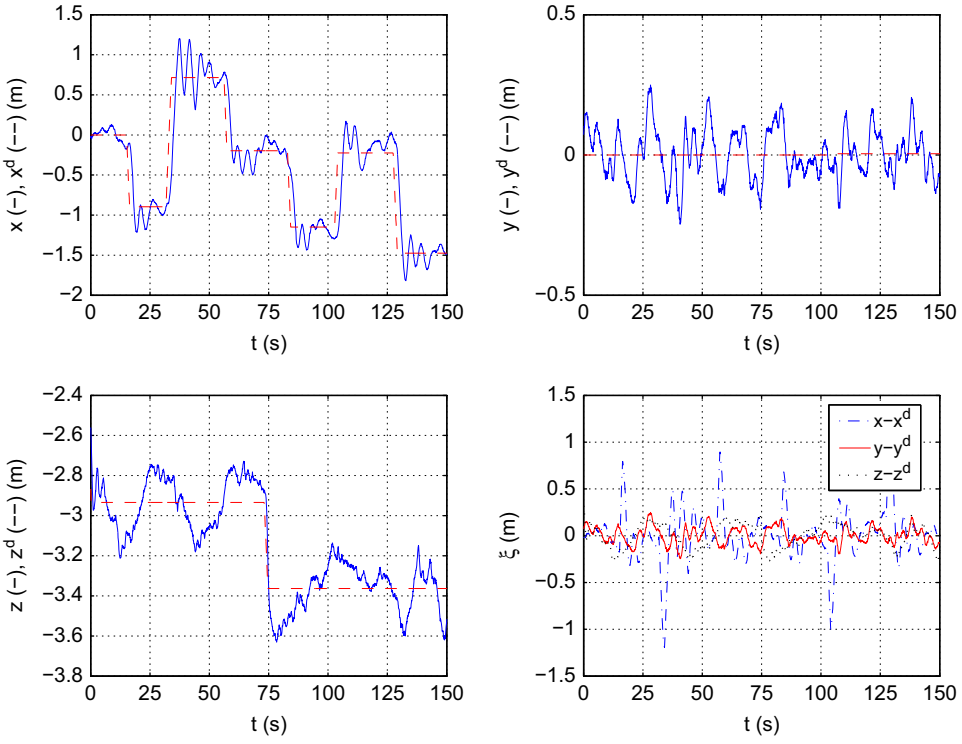


**Fig. 7.** Position coordinates and position error.

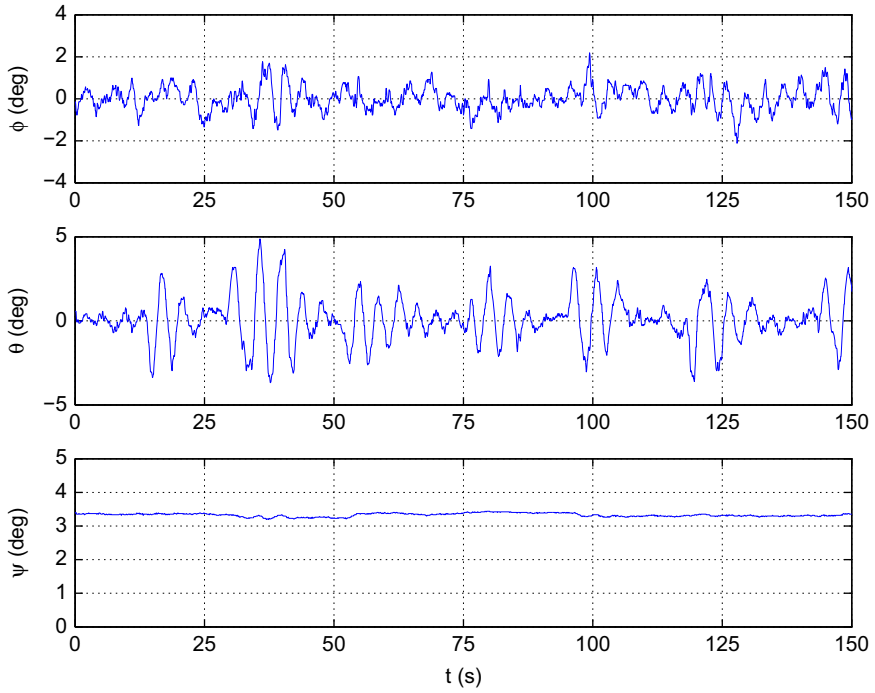


**Fig. 8.** Attitude angles.

has been proposed for position stabilization, assuming that no measurement of the linear velocity of the vehicle is available. Time-scale separation of the proposed control scheme and stability analysis has been addressed by singular perturbation theory. Simulation results and experimental results achieved on a X4-flyer miniature UAV have been finally proposed to illustrate the good performance obtained by the controller.

## Appendix A. Computation of the desired angular velocity

A method to compute $\Omega^d$ from the control vector $\mathcal{T}R^de_3$ is presented here. From (12) we get

$$\frac{d}{dt}(R^de_3)=\dot{R}^de_3=R^d\Omega^d_\times e_3 \tag{A.1}$$

and then

$$\Omega^d_\times e_3=(R^d)^T\frac{d}{dt}(R^de_3) \tag{A.2}$$

To compute the time derivative of $R^de_3$, let us define

$$N=\mathcal{T}R^de_3 \tag{A.3}$$

so that we get

$$R^de_3=\frac{N}{\sqrt{N^TN}} \tag{A.4}$$

The time derivative of $R^de_3$ is given by

$$\frac{d}{dt}(R^de_3)=\frac{\dot{N}\sqrt{N^TN}-\frac{NN^T\dot{N}}{\sqrt{N^TN}}}{N^TN}=\frac{1}{\sqrt{N^TN}}\left(I_d-\frac{NN^T}{N^TN}\right)\dot{N} \tag{A.5}$$

Therefore, we have

$$\frac{d}{dt}(R^de_3)=\frac{1}{\mathcal{T}}\{I_d-R^de_3e_3^T(R^d)^T\}\frac{d}{dt}(\mathcal{T}R^de_3) \tag{A.6}$$

Defining the projector

$$\Pi_{e_3}=I_d-e_3e_3^T \tag{A.7}$$

Eq. (A.2) can be restated as

$$\Omega^d_\times e_3=\begin{bmatrix}\Omega^d_2\\-\Omega^d_1\\0\end{bmatrix}=\frac{1}{\mathcal{T}}\Pi_{e_3}(R^d)^T\frac{d}{dt}(\mathcal{T}R^de_3) \tag{A.8}$$

Considering the stabilization of the UAV around a fixed point, the third component $\Omega^d_3$ of the vector $\Omega^d$ is chosen to be identically zero, and we have $\psi^d(t)=\psi^d(0)$, for a given initial yaw $\psi^d(0)$.

## References


Bertrand, S., Hamel, T., & Piet-Lahanier, H. (2007). Trajectory tracking of an unmanned aerial vehicle model using partial state feedback. In *European control conference*. Kos, Greece.

Bertrand, S., Hamel, T., & Piet-Lahanier, H. (2008). Stability analysis of an UAV controller using singular perturbation theory. In *Proceedings of the 17th IFAC world congress* (pp. 5706–5711). Seoul, Korea.

Bouabdallah, S., Noth, A., & Siegwart, R. (2004). PID vs LQ control techniques applied to an indoor micro quadrotor. In *Proceedings of the 2004 IEEE/RSJ international conference on intelligent robots and systems* (Vol. 3, pp. 2451–2456). Sendai, Japan.

Bouabdallah, S., & Siegwart, R. (2005). Backstepping and sliding-mode techniques applied to an indoor micro quadrotor. In *Proceedings of the 2005 IEEE international conference on robotics and automation* (pp. 2259–2264). Barcelona, Spain.

Budiyono, A., & Wibowo, S. S. (2007). Optimal tracking controller design for a small scale helicopter. *Journal of Bionic Engineering*, *4*(4), 271–280.

Burg, T., Dawson, D., Hu, J., & de Queiroz, M. (1996). An Adaptive partial state-feedback controller for RLED robot manipulators. *IEEE Transactions on Automatic Control*, *41*(7), 1024–1030.

Burg, T., Dawson, D., & Vedagarbha, P. (1997). A redesigned DCAL controller without velocity measurements: Theory and demonstration. *Robotica*, *15*, 337–346.

Dixon, W. E., Zergeroglu, E., Dawson, D. M., & Hannan, M. W. (2000). Global adaptive partial state feedback tracking control of rigid-link flexible-joints robots. *Robotica*, *18*, 325–336.

Dzul, A., Hamel, T., & Lozano, R. (2003). Modélisation et Commande Non Linéaire pour un Hélicoptère Birotor Coaxial. *Journal Européen des Systémes Automatisés*, *37*(10), 1277–1295.

Esteban, S., Aracil, J., & Gordillo, F. (2005). Three-time scale singular perturbation control for a radio-control helicopter on a platform. In *AIAA atmospheric flight mechanics conference and exhibit*. San Francisco, USA.

Esteban, S., Gordillo, F., & Aracil, J. (2007). Lyapunov based stability analysis of a three-time scale model for a helicopter on a platform. In *17th IFAC symposium on automatic control in aerospace*. Toulouse, France.

Frazzoli, E., Dahleh, M. A., & Feron, E. (2000). Trajectory tracking control design for autonomous helicopters using a backstepping algorithm. In *2000 American control conference*. Chicago, USA.

Guenard, N., Hamel, T., & Eck, L. (2006). Control laws for the tele operation of an unmanned aerial vehicle known as a X4-Flyer. In *Proceedings of the 2006 IEEE/RSJ international conference on intelligent robots and systems* (pp. 3249–3254). Beijing, China.

Hamel, T., & Mahony, R. (2004). Pure 2D visual control for a class of under-actuated dynamic systems. In *Proceedings of the 2004 IEEE international conference on robotics and automation* (Vol. 3, pp. 2229–2235). New Orleans, USA.

Hamel, T., Mahony, R., Lozano, R., & Ostrowski, J. (2002). Dynamic modeling and configuration stabilization for a X4-Flyer. In *15th triennial IFAC world congress*. Barcelona, Spain.

Heiges, M. W., Menon, P. K., & Schrage, D. P. (1989). Synthesis of a helicopter full authority controller. In *Proceedings of the AIAA guidance, navigation and control conference* (pp. 207–213). Boston, USA.

Khalil, H. K. (1992). *Nonlinear systems* (1st ed.). Macmillan.

Kokotovic, P. V., Khalil, H. K., & O'Reily, J. (1986). *Singular perturbation methods in control: Analysis and design*. Academon Press.

Koo, T. J., & Sastry, S. (1998). Output tracking control design of a helicopter model based on approximate linearization. In *Proceedings of the 37th IEEE conference on decision and control*. Tampa, Florida, USA.

Kundak, N., & Mettler, B. (2007). Experimental framework for evaluating autonomous guidance and control algorithms for agile aerial vehicles. In *Proceedings of the European control conference 2007* (pp. 293–300). Kos, Greece.

Mahony, R., & Hamel, T. (2004). Robust trajectory tracking for a scale model autonomous helicopter. *International Journal of Robust and Nonlinear Control*, *14*, 1035–1059.

Naidu, D. S., & Calise, A. J. (2001). Singular perturbations and time scales in guidance and control of aerospace systems: A survey. *Journal of Guidance, Control, and Dynamics*, *24*(6), 1057–1078.

Njaka, C. E., & Menon, P. K. (1994). Towards an advanced nonlinear rotorcraft flight control system design. In *13th AIAA/IEEE digital avionics systems conference*. Phoenix, USA.

Pflimlin, J. M., Hamel, T., Souères, P., & Mahony, R. (2006). A hierarchical control strategy for the autonomous navigation of a ducted fan VTOL UAV. In *Proceedings of the 2006 IEEE international conference on robotics and automation* (pp. 2491–2496). Orlando, USA.

Valenti, M., Bethke, B., Fiore, G., How, J. P., & Feron, E. (2006). Indoor multi-vehicle flight testbed for fault detection, isolation, and recovery. In *AIAA guidance, navigation, and control conference and exhibit*. Keystone, USA.

Waslander, S. L., Hoffman, G. M., Jang, J. S., & Tomlin, C. J. (2005). Multi-agent quadrotor testbed control design: Integral sliding mode vs. reinforcement learning. In *Proceedings of the 2005 IEEE/RSJ international conference on intelligent robots and systems* (pp. 3712–3717). Edmonton, Canada.